

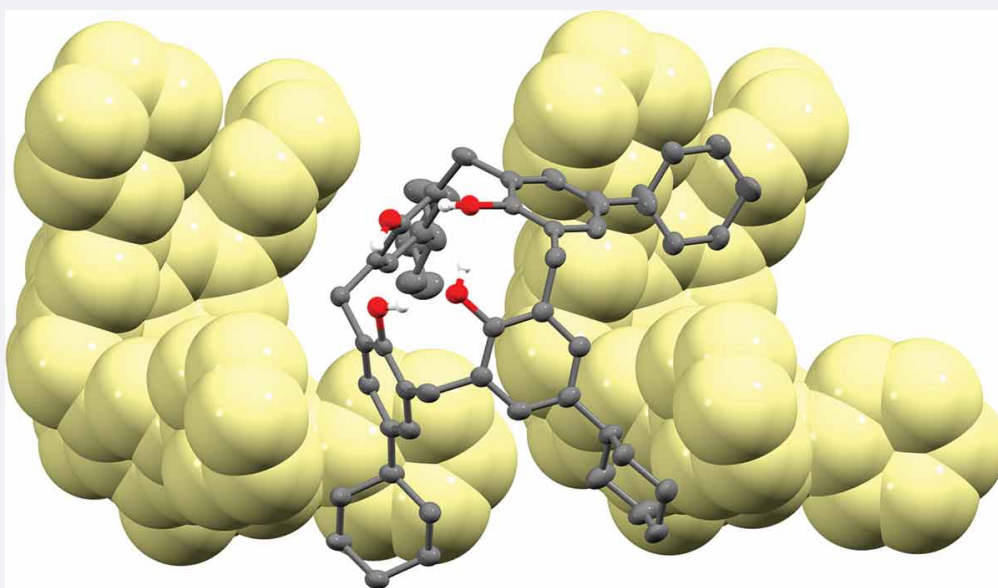
Structure, derivatisation, and metal complexation of p-cyclohexylcalix[4]arene

Chao Shen^a, Rene Z. H. Phe^a, Isabella Fong^a, Alexandre N. Sobolev ^b, Mauro Mocerino ^a, Massimiliano Massi ^a, and Mark I. Ogden ^a

^a School of Molecular and Life Sciences, Curtin University, Perth, WA, Australia ^b School of Molecular Sciences, M310, University of Western Australia, Perth, WA, Australia

ABSTRACT

Driven by an interest in the impact of the para-substituent of calix[4]arenes on metal complexation and structural chemistry, studies of p-cyclohexylcalix[4]arene (L) have been carried out. The 1:1 dichloromethane and dimethylformamide solvates were found to be isostructural, and different to the typical bilayer structure often observed for p-t-butylcalix[4]arene solvates. The methanol solvate, in contrast, does form a bilayered structure but is also a 1:1 solvate, unlike the p-t-butylcalix[4]arene·2MeOH system. Lanthanoid complexation was investigated, resulting in the structural characterisation of two different DMF solvates of a 2:2 dimeric europium complex, $\text{Eu}_2(\text{L}-3\text{H})_2(\text{DMF})_4$. A tetrazole derivative, 5,11,17,23-tetracyclohexyl-25,27-dihydroxy-26,28-bis(tetrazole-5-ylmethoxy)calix[4]arene, has been synthesised via the intermediate 5,11,17,23-tetracyclohexyl-25,27-dihydroxy-26,28-dicyanomethoxycalix[4]arene, with the latter compound being structurally characterised. Attempts to isolate lanthanoid clusters supported by the tetrazole derivative under conditions known to form Ln_{19} clusters with the p-t-butyl analogue were unsuccessful, resulting only in isolation of the ligand from the reaction mixture.



ARTICLE HISTORY

Received 1 June 2021
Accepted 20 July 2021

KEYWORDS

Calixarene, tetrazole, lanthanide, crystal, structure

CONTACT Mark I. Ogden  m.ogden@curtin.edu.au School of Molecular and Life Sciences, Curtin University, 35 Stirling Hwy, Perth, 6845, Australia

© 2021 Informa UK Limited, trading as Taylor & Francis Group

Introduction

Calixarenes, and particularly calix[4]arenes, are well established as a readily modified macrocyclic framework which can be substituted at the phenol moieties, the position para to the phenol group, and the linking methylene carbon atoms [1]. Recently we have been probing the impact of the nature of the para substituent on the formation and structure of lanthanoid complexes of a series of calix[4]arene bis-substituted at the lower rim with tetrazole moieties. The p-t-butylcalix[4]arene bis-tetrazole was found to form remarkable Ln19 or Ln12 'bottlebrush' clusters supported by the calixarene along with carboxylate coligands [2]. Under the same reaction conditions, the related p-H and p-allyl tetrazole-functionalised calixarenes formed only mononuclear metal complexes in the solid state and solution [3]. In this instance at least, it appears that the para substituent has a profound impact on the nature of the metal complexes formed.

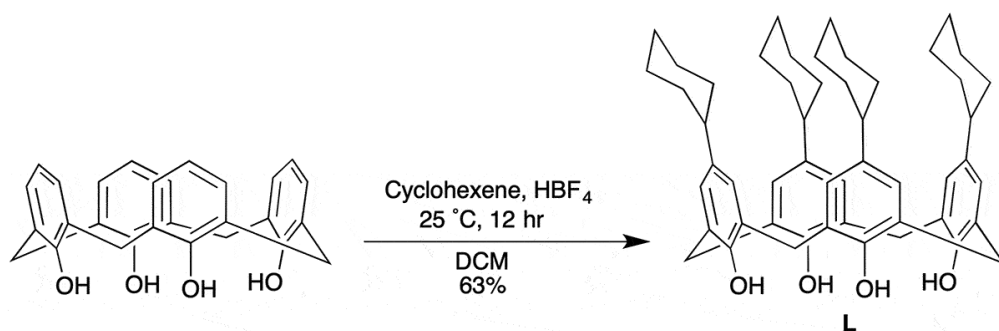
This observation prompted us to target other related derivatives, and an attractive option was the p-cyclohexyl substituted system. First reported by Arduini et al. in 1992, p-cyclohexylcalix[4]arene was synthesised by the reaction of cyclohexene with calix[4]arene in the presence of tetrafluoroboric acid [4]. In the context of the target bis-tetrazole functionalised calixarene, this p-cyclohexyl derivative has an increase in lipophilicity of the para-substituent relative to the t-butyl group, rather than the decrease of the p-H and p-allyl derivatives, which we proposed might better support the formation of the bottlebrush clusters.

In examining the literature to determine how the p-cyclohexyl groups might impact on the solid-state behaviour of calixarene derivatives, we found that there are surprisingly few crystal structures of calixarenes fully substituted at the upper rim by cyclohexyl groups. Examples are limited to two solvates of a lower rim biscrown-3 derivative [5,6], and a tungsten complex of p-cyclohexylcalix[4]arene [7]. There are three other examples that are 1,3-bis substituted at the upper rim with cyclohexyl groups, with a bridging chain between the other two para positions [8,9]. Given this lack of structurally characterised p-cyclohexylcalixarene derivatives, in the course of this work we aimed to carry out crystal structure determinations of the parent calixarene, derivatives, and lanthanoid complexes where possible.

We report here the first crystal structures of p-cyclohexylcalix[4]arene as dichloromethane, dimethylformamide, and methanol solvates, along with a dinuclear 2:2 europium complex of this ligand. The syntheses of the phenol rim bis-substituted cyanomethoxy and tetrazole-5-ylmethoxy derivatives are also described, as well as the results of attempted syntheses of lanthanoid bottlebrush clusters supported by the tetrazole-functionalised calixarene.

Results and discussion

Synthesis and structural studies of p-cyclohexylcalix[4]arene



Scheme 1. Synthesis of p-cyclohexylcalix[4]arene, **L**.

The cyclohexyl-substituted calix[4]arene **L** was readily synthesised following the literature procedure [4], with a modification to the purification procedure (Scheme 1). Instead of column chromatography, the crude product was triturated in acetone to remove excess cyclohexene, giving a product sufficiently pure for subsequent use. ^1H and ^{13}C NMR spectra of the product were consistent with the literature [4]. Crystals suitable for X-ray structure determination were grown by slow evaporation of a solution of the calixarene in 1:1 dichloromethane:methanol.

The structure elucidation shows that the calixarene assumed the typical cone conformation in the solid state, stabilised by hydrogen bonds between the phenol O atoms (Figure 1(a)). The calixarene has quasi 4-fold symmetry with the angles between the methylene C4 plane and aromatic rings being: ring 1, 56.3; ring 2, 54.6; ring 3, 52.9; ring 4, 57.7°. The crystal structure is orthorhombic in the $\text{P2}_1\text{2}_1\text{2}_1$ space group, with the macrocycles packed along a 2-fold screw axis as shown in Figure 2.

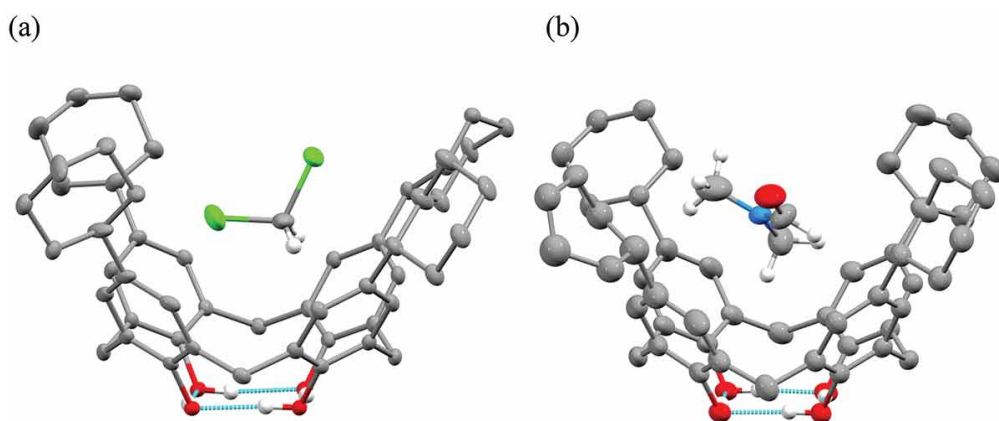


Figure 1. The molecular structures of (a) p-cyclohexylcalix[4]arene- CH_2Cl_2 , and (b) p-cyclohexylcalix[4]arene-DMF showing the intramolecular hydrogen bonding, with one component of the disordered atoms and hydrogen atoms other than phenol OH and solvent guest H omitted for clarity. Ellipsoids are shown at 25% probability

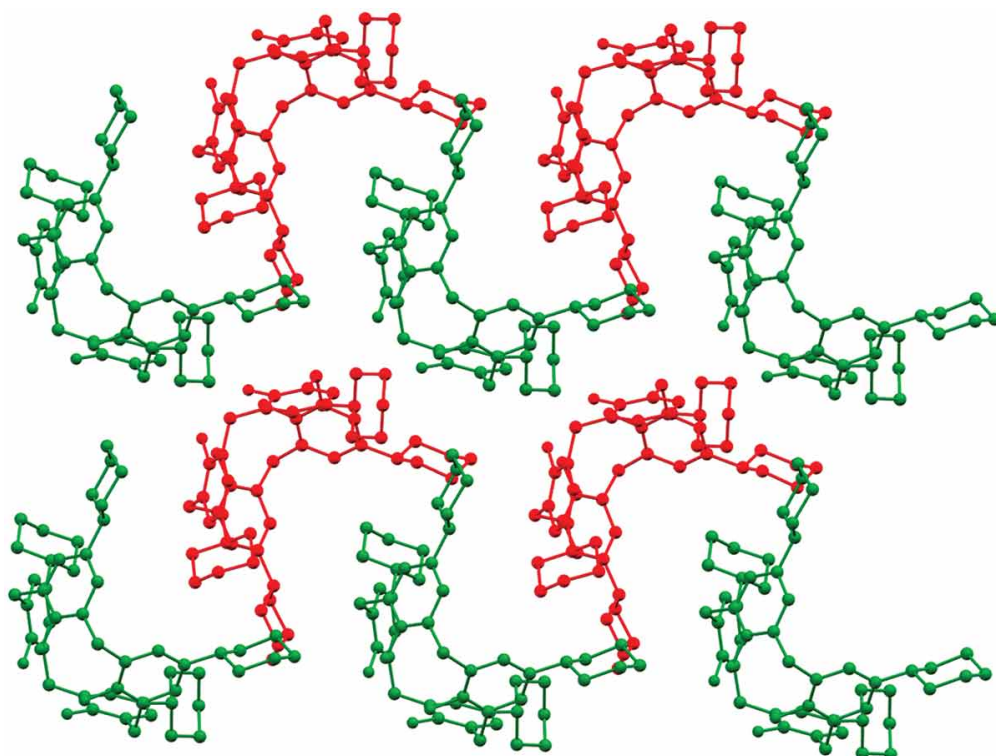


Figure 2. Packing of p-cyclohexylcalix[4]arene molecules in the CH_2Cl_2 solvate showing molecules alternating green and red along a horizontal 2-fold screw axis

During the course of attempts to crystallise lanthanoid complexes of this calixarene, two other 1:1 solvates crystallised and were structurally characterised. The dimethylformamide (DMF) solvate is isostructural with the dichloromethane solvate, with the DMF guest oriented with the methyl groups directed into the cavity (angles between the methylene C4 plane and aromatic rings being: ring 1, 55.4; ring 2, 54.6; ring 3, 53.1; ring 4, 56.4°), [Figure 1\(b\)](#). In both of these solvates, any detailed analysis of the guest solvent interactions with the calixarene cavity is confounded by disorder. The methanol solvate in contrast crystallises as a triclinic $P\bar{1}$ bilayered structure that is more similar to many of the solvates of p-t-butylcalix[4]arene ([Figure 3](#)). The macrocycle again has quasi 4-fold symmetry, and is less distorted than the previous two structures with angles between the methylene C4 plane and aromatic rings being: ring 1, 54.9; ring 2, 56.0; ring 3, 56.4; ring 4, 55.8°.

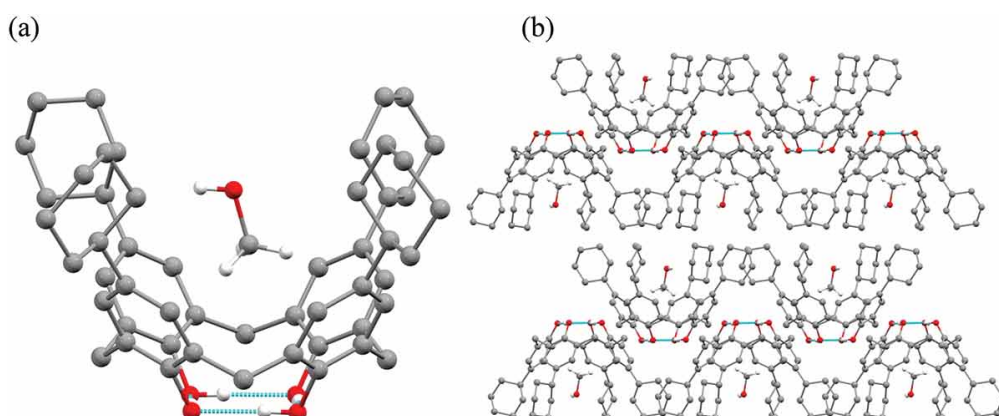


Figure 3. The structure of p-cyclohexylcalix[4]arene-MeOH. (a) The molecular structure showing the orientation of the methanol guest molecule, and (b) the bilayer packing viewed along the a-axis

These structures can be compared to the equivalent p-t-butylcalix[4]arene systems for DMF [10] and methanol [11] solvates. Both crystallise as tetragonal $P4/n$ bilayered

structures, as commonly found for solvates of this calixarene, with the calixarenes having crystallographic 4-fold symmetry. The DMF system is a 1:1 solvate with a similar guest orientation to that observed here, whereas the methanol solvate is a 1:2 system with one methanol deeply embedded in the cavity, and a hydrogen bond linking to a second methanol in the vicinity of the t-butyl substituents.

While more p-cyclohexylcalix[4]arene solvate structures will be needed to determine any trends in the impact on crystal packing of the cyclohexyl substituents, the results obtained here do confirm that the structures obtained are likely to be different to those observed with the t-butyl substituted analogues.

Lanthanoid complexation with p-cyclohexylcalix[4]arene

It has been shown that p-t-butylcalix[4]arene can support lanthanoid clusters where simple changes in the solvent mixture used can change the clusters formed from dimers [12], to octahedral hexanuclear clusters [13]. Attempts were made to isolate hexanuclear europium clusters using the literature procedure, substituting in p-cyclohexylcalix[4]arene, however no crystalline materials were isolated. A range of conditions were then tested, varying the metal:ligand:base ratio, and solvent mixtures (see SI). Europium was used throughout these tests, as binding to the phenolate O atoms results in an orange complex due to a charge transfer absorption band, making identification of metal complexes straightforward [14]. During the course of these experiments, the methanol and DMF solvates of **L** discussed above were serendipitously crystallised in low yield (Table S1). In two cases, metal complexes were crystallised (Table S1), and structural characterisation showed that both were different DMF solvates of essentially identical dimeric 2:2 europium complexes, $\text{Eu}_2(\text{L}-3\text{H})_2(\text{DMF})_4 \cdot 6/7\text{DMF}$, very similar to that reported for the analogous p-t-butylcalix[4]arene structure (Figure 4) [12].

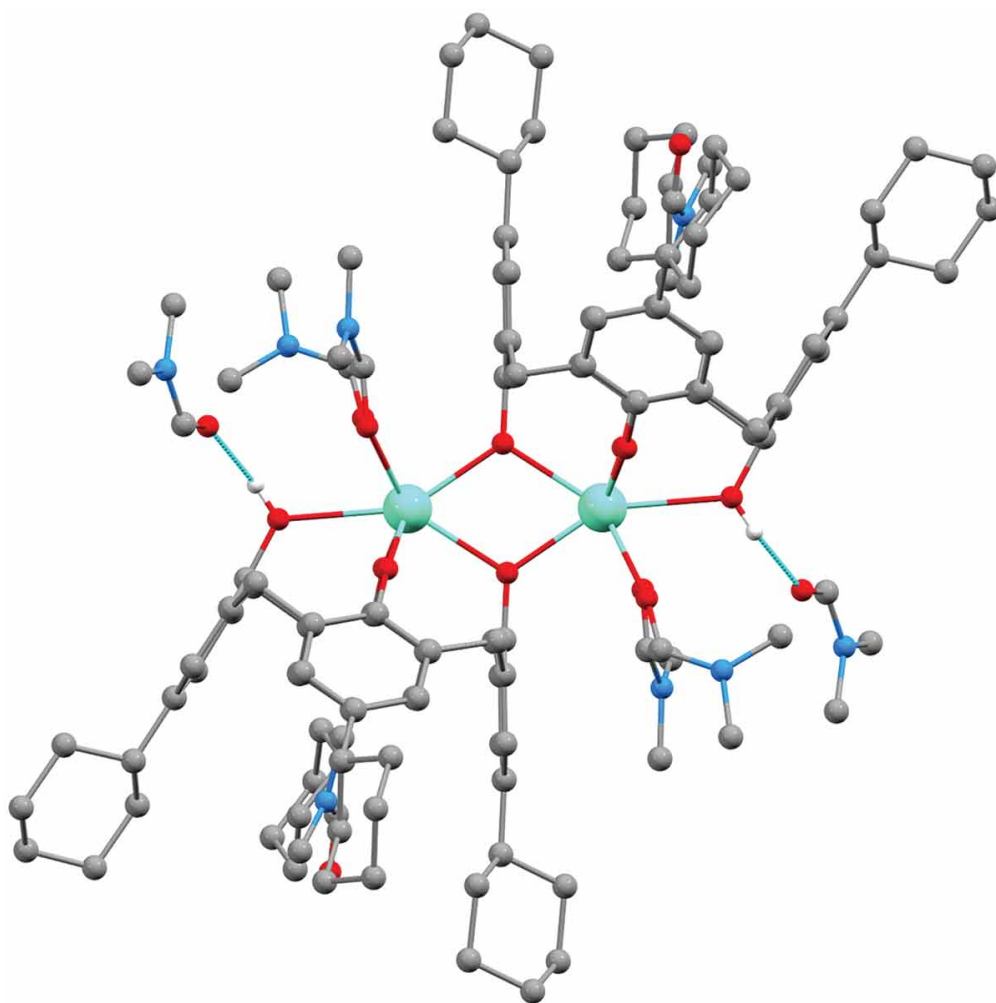
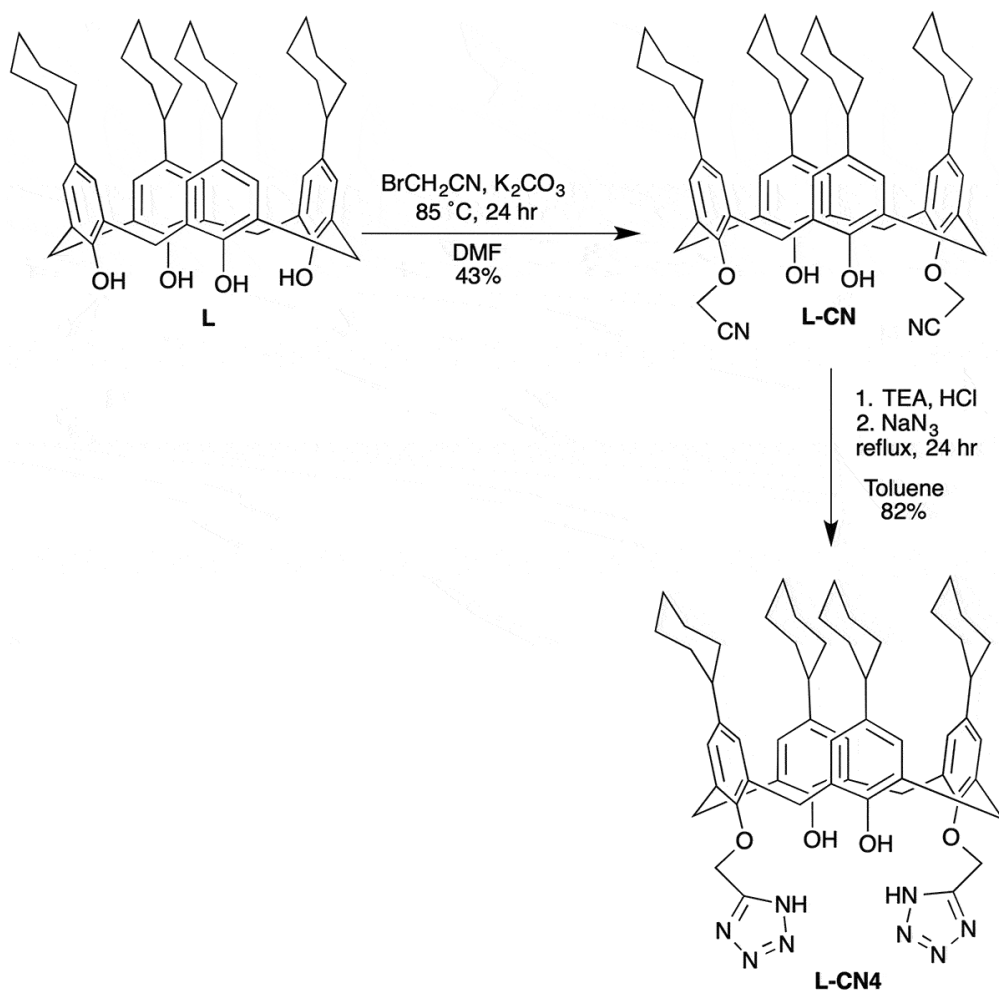


Figure 4. The dimer formed in the europium complex of p-cyclohexylcalix[4]arene, $\text{Eu}_2(\text{L}-3\text{H})_2(\text{DMF})_4 \cdot 7\text{DMF}$, (**EuL-7DMF**) showing the DMF molecules situated in the cavity of the calixarenes, and DMF molecules forming hydrogen bonds to the protonated O atoms

These results indicate that p-cyclohexylcalix[4]arene can form similar lanthanoid complexes to p-t-butylcalix[4]arene in at least the case of the dimeric complex found here. In general, however, the solubility of the cyclohexyl derivative appears to be low enough under the reaction conditions that ligand crystallisation can be favoured over the metal complex.

Tetrazolyl-functionalisation of p-cyclohexylcalix[4]arene

The tetrazole substituted derivative of p-cyclohexylcalix[4]arene was synthesised as shown in [Scheme 2](#), following the same approach as reported for analogous systems [\[3,15\]](#). Both the intermediate nitrile derivative and the final product were isolated in acceptable yields and purity.



Scheme 2. Synthesis of bis-tetrazole functionalised p-cyclohexylcalix[4]arene, **L-CN4**

While the tetrazole-functionalised product **L-CN4** could not be crystallised in a form appropriate for structure determination to date, the intermediate nitrile derivative **L-CN** forms well-shaped crystals upon slow evaporation of a dichloromethane/methanol solution, and the molecular structure is shown in Figure 5. A molecule of dichloromethane is found in the cavity of the calixarene, in this case with no disorder. The H atoms are directed into the cavity and oriented consistent with a CH ... π interaction with the more vertical aromatic rings (C ... centroid, 3.449 Å). The macrocycle adopts a typical 'pinched' cone conformation, commonly observed for bis-substituted calix[4]arene systems, with 2-fold rotational symmetry. The angles of the two unique aromatic rings relative to the C4 methylene plane are 40.9 and 73.7°.

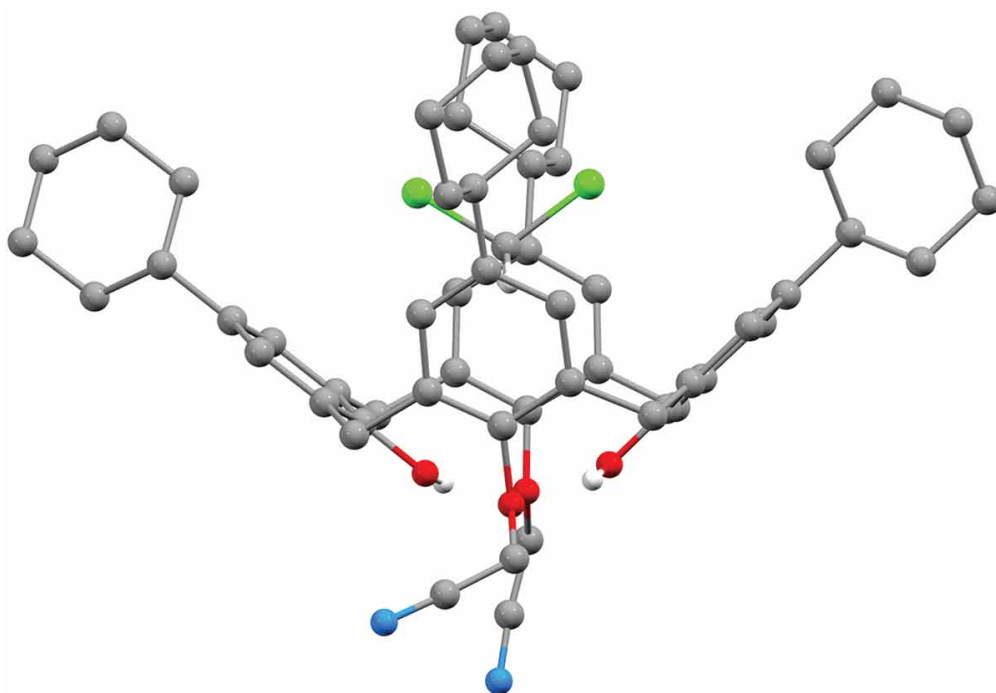


Figure 5. The molecular structure of 5,11,17,23-tetracyclohexyl-25,27-dihydroxy-26,28-dicyanomethoxycalix[4]arene, **L-CN**, excluding disordered components and hydrogen atoms aside from phenol and solvent H atoms

The crystal packing of this trigonal structure results in two distinct types of cylindrical pores running in the *c*-direction (Figure 6), one lined with disordered nitrile moieties, and the other with cyclohexyl groups. The solvent molecules in these pores were heavily disordered and could not be modelled. The analogous bis-nitrile functionalised *p*-*t*-butylcalix[4]arene has been reported to crystallise with a similar ‘pinched’ molecular conformation, but without any included solvent, and in a bilayer structure [16,17]. This again indicates that the cyclohexyl-substituted calixarenes may be worthy of more extensive investigation to probe the impact on crystal packing.

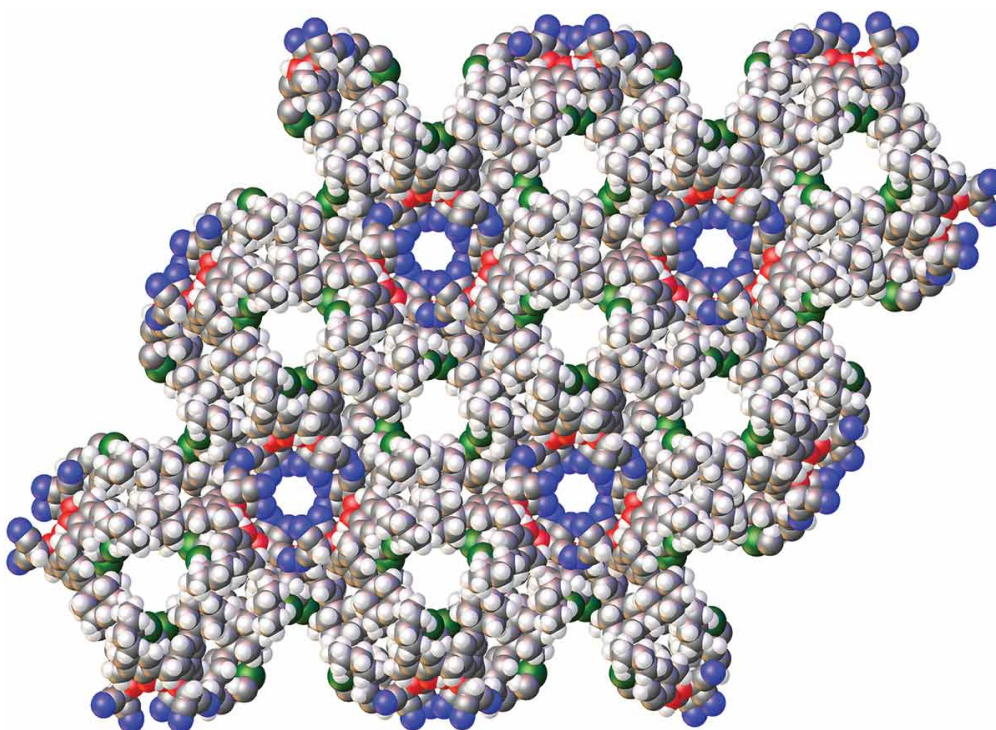


Figure 6. Crystal packing of 5,11,17,23-tetracyclohexyl-25,27-dihydroxy-26,28-dicyanomethoxycalix[4]arene, **L-CN**, as a space-filling model with all disordered components included,

viewed down the c-axis

Reaction of the bis-tetrazole derivative with lanthanoids under conditions reported to form the large Ln bottlebrush clusters [2], resulted only in the precipitation of the ligand. In this case, the presence of water in the reaction mixture and the greater hydrophobicity of the cyclohexyl derivative compared to the t-butyl derivative are likely to be contributing to the precipitation of the ligand rather than any metal complex.

Conclusions

This work has shown that p-cyclohexylcalix[4]arene solvates differ in structure from similar p-t-butylcalix[4]arene systems, although more structures will need to be determined to extract underlying trends. This may broaden the understanding and potential applications of these systems in the solid state, for example extending the accessible properties of calixarenes [18,19] behaving as intrinsically porous materials [20]. Similarly, metal coordination studies of the p-cyclohexyl substituted macrocycles show different behaviours to the related t-butyl functionalised systems. This appears to be related in part to the lower solubility, under the reaction conditions, leading to the crystallisation of the ligand rather than metal complex in a number of cases. The dimeric europium complex of the parent calixarene was successfully characterised, showing that in some cases similar complexes can be formed with both t-butyl and cyclohexyl substituted calix[4]arenes.

Experimental

The syntheses and characterisation of the calixarene derivatives, the crystallisation conditions trialled, and additional structural details, are reported in the supplementary information.

Crystallography

Full spheres of CCD area-detector diffractometer data were measured from single crystals using Oxford Diffraction Xcalibur-S or Gemini-R Ultra CCD diffractometer at $T = 100$ [2] K with monochromatic MoK α ($\lambda = 0.71073$ Å) or CuK α ($\lambda = 1.54178$ Å) radiation. Data were corrected for Lorentz and polarisation effects, absorption correction applied using multiple symmetry equivalent reflections. The structures were solved by direct methods and refined against F^2 with full-matrix least-squares using the programs suit SHELX [21]. Anisotropic displacement parameters were employed for the non-hydrogen atoms. All hydrogen atoms were added at calculated positions and refined by use of a riding model with isotropic displacement parameters based on those of the parent atom. Crystallographic data for the structures reported in this paper have been deposited at the Cambridge Crystallographic Data Centre. Copies of data with CCDC numbers 2,083,764–2,083,769 can be obtained free of charge via <https://www.ccdc.cam.ac.uk/structures/>, or from the Cambridge Crystallographic Data Centre, 12 Union Road, Cambridge CB2 1EZ, U.KCB21EZ, UK (fax +441,223,336,033; email deposit@ccdc.cam.ac.uk)

Crystal data for L•CH₂Cl₂: C₅₂H₆₄O₄•CH₂Cl₂

C₅₃H₆₆Cl₂O₄, $M = 837.95$, colourless plate, $0.33 \times 0.28 \times 0.06$ mm³, orthorhombic, space group P2₁2₁2₁ (No. 19), $a = 13.6033$ [1], $b = 13.9929$ [1], $c = 23.6483$ [1] Å, $V = 4501.45$ [5] Å³, $Z = 4$, $D_c = 1.236$ g/cm³, $\mu = 1.644$ mm⁻¹. $F_{000} = 1800$, CuK α radiation, $2\theta_{\max} = 134.6^\circ$, 101,660 reflections collected, 8074 unique ($R_{\text{int}} = 0.0518$). Final

GooF = 1.002, R1 = 0.0631, wR2 = 0.1509, R indices based on 7581 reflections with $I > 2\sigma(I)$, $|\Delta\rho|_{\max} = 1.00$ [6] e Å⁻³, 558 parameters, 13 restraints. Absolute structure parameter = 0.001 [5] [22]. CCDC number 2,083,764.

Crystal data for L•DMF: C₅₂H₆₄O₄•C₃H₇NO

C₅₅H₇₁NO₅, M = 826.12, colourless plate, 0.307 × 0.280 × 0.186 mm³, orthorhombic, space group P2₁2₁2₁ (No. 19), a = 14.1049 [1], b = 14.2242 [2], c = 22.8813 [2] Å, V = 4590.70 [8] Å³, Z = 4, D_c = 1.195 g cm⁻³, μ = 0.582 mm⁻¹. F₀₀₀ = 1792, CuK_α radiation, 2θ_{max} = 134.7°, 101,445 reflections collected, 8205 unique (R_{int} = 0.0672). Final GooF = 1.002, R1 = 0.0849, wR2 = 0.1812, R indices based on 6488 reflections with $I > 2\sigma(I)$, $|\Delta\rho|_{\max} = 0.74$ [5] e Å⁻³, 608 parameters, 219 restraints. Absolute structure parameter = 0.01 [8] [22]. CCDC number 2083765.

Crystal data for L•MeOH: C₅₂H₆₄O₄•CH₄O

C₅₃H₆₈O₅, M = 785.07, colourless prism, 0.186 × 0.143 × 0.123 mm³, triclinic, space group P $\bar{1}$ (No. 2), a = 12.5820 [6], b = 12.8275 [6], c = 15.5306 [6] Å, α = 83.946 [3], β = 70.231 [4], γ = 89.726 [4]°, V = 2344.41 [19] Å³, Z = 2, D_c = 1.112 g cm⁻³, μ = 0.540 mm⁻¹. F₀₀₀ = 852, CuK_α radiation, 2θ_{max} = 135.2°, 51,469 reflections collected, 8353 unique (R_{int} = 0.0913). Final GooF = 1.000, R1 = 0.1144, wR2 = 0.2393, R indices based on 4347 reflections with $I > 2\sigma(I)$, $|\Delta\rho|_{\max} = 1.16$ [7] e Å⁻³, 572 parameters, 201 restraints. CCDC number 2,083,766.

Crystal data for EuL•7DMF: C₁₁₆H₁₄₈Eu₂N₄O₁₂, 7(C₃H₇NO)

C₁₃₇H₁₉₇Eu₂N₁₁O₁₉, M = 2605.96, yellow needle, 0.243 × 0.201 × 0.140 mm³, triclinic, space group P $\bar{1}$ (No. 2), a = 12.9282 [2], b = 13.9847 [2], c = 21.2223 [3] Å, α = 73.377 [1], β = 89.778 [1], γ = 64.370 [2]°, V = 3282.76 [10] Å³, Z = 1, D_c = 1.318 g cm⁻³, μ = 1.015 mm⁻¹. F₀₀₀ = 1374, MoK_α radiation, 2θ_{max} = 64.5°, 70,022 reflections collected, 21,568 unique (R_{int} = 0.0319). Final GooF = 1.001, R1 = 0.0431, wR2 = 0.1113, R indices based on 19,220 reflections with $I > 2\sigma(I)$, $|\Delta\rho|_{\max} = 1.8$ [1] e Å⁻³, 804 parameters, 79 restraints. CCDC number 2,083,767.

Crystal data for EuL•6DMF: C₁₁₆H₁₆₀N₄O₁₂Eu₂, 6(C₃H₇NO) + solvent

C₁₃₄H₂₀₂Eu₂N₁₀O₁₈, M = 2534.88, yellow needle, 0.303 × 0.116 × 0.052 mm³, triclinic, space group P $\bar{1}$ (No. 2), a = 12.9144 [8], b = 13.8959 [6], c = 21.1781 [8] Å, α = 73.648 [4], β = 89.857 [4], γ = 64.471 [5]°, V = 3259.6 [3] Å³, Z = 1, D_c = 1.291 g cm⁻³, μ = 7.344 mm⁻¹. F₀₀₀ = 1336, CuK_α radiation, 2θ_{max} = 134.9°, 32,395 reflections collected, 11,549 unique (R_{int} = 0.0704). Final GooF = 1.001, R1 = 0.0741, wR2 = 0.1673, R indices based on 8908 reflections with $I > 2\sigma(I)$, $|\Delta\rho|_{\max} = 1.53$ [9] e Å⁻³, 774 parameters, 101 restraints. CCDC number 2,083,768.

Crystal data for L-CN•CH₂Cl₂: C₅₆H₆₆N₂O₄, CH₂Cl₂ + solvent

C₅₇H₆₈Cl₂N₂O₄, M = 916.03, colourless needle, 0.35 × 0.28 × 0.19 mm³, trigonal, space group P $\bar{3}$ 1c (No. 163), a = 26.1274 [1] b = 26.1274 [1], c = 14.2499 [1] Å, V = 8424.32 [9] Å³, Z = 6, D_c = 1.083 g/cm³, μ = 1.368 mm⁻¹. F₀₀₀ = 2940, CuK_α radiation, 2θ_{max} = 134.6°, 91,165 reflections collected, 5044 unique (R_{int} = 0.0362). Final GooF = 1.005, R1 = 0.0751, wR2 = 0.1697, R indices based on 4531 reflections with $I > 2\sigma(I)$, $|\Delta\rho|_{\max} = 1.32$ [7] e Å⁻³, 301 parameters, 2 restraints. CCDC number 2,083,769.

Acknowledgments

We acknowledge use of the facilities and scientific and technical assistance of the Australian Microscopy and Microanalysis Research Facility at the Centre for Microscopy, Characterisation, and

Analysis, The University of Western Australia, a facility funded by the University, State and Commonwealth Governments. The first author is funded by the China Scholarship Council (CSC) from the Ministry of Education of P.R. China.

Disclosure statement

No potential conflict of interest was reported by the author(s).

Funding

This work was supported by the China Scholarship Council.

Supplementary material

Supplemental data for this article can be accessed [here](#).

References

- [1] Gutsche CD. Calixarenes: an Introduction. 2nd ed. Cambridge: RSC Publishing; 2008.
- [2] D' Alessio D, Sobolev AN, Skelton BW, et al. Lanthanoid "Bottlebrush" clusters: remarkably elongated Metal–Oxo core structures with controllable lengths. *J. Am. Chem. Soc.* 2014;136(43):15122–15125.
- [3] Phe RZH, Skelton B, Massi M, et al. Influence of the para -Substituent in lanthanoid complexes of Bis-Tetrazole-Substituted Calix[4]arenes. *Eur. J. Inorg. Chem.* 2020;2020(1):94–100.
- [4] Arduini A, Pochini A, Rizzi A, et al. Extension of the hydrophobic cavity of calix[4]arene by "upper rim" functionalization. *Tetrahedron.* 1992;48(5):905.
- [5] Arduini A, McGregor WM, Paganuzzi D, et al. Rigid cone calix[4]arenes as π -donor systems: complexation of organic molecules and ammonium ions in organic media. *J. Chem. Soc., Perkin Trans. 2* 1996;(5):839–846.
- [6] Arduini A, Nachtigall FF, Pochini A, et al. Calix[4]arene cavitands: a solid state study on the interactions of their aromatic cavity with neutral organic guests characterised by acid CH_3 or CH_2 groups. *Supramol. Chem.* 2000;12(3):273–291.
- [7] Arduini A, Massera C, Pochini A, et al. Organic guests inclusion by tungsten-calix[4]arene hosts. *New J. Chem.* 2006;30(6):952–958.
- [8] Berger B, Bohmer V, Paulus E, et al. Bicyclocalix[4]arenes. *Angew. Chem. Int. Ed.* 1992;31(1):96–99.
- [9] Paulus E, Bohmer V, Goldmann H, et al. The crystal and molecular structure of two calix[4]arenes bridged at opposite para positions. *J. Chem. Soc. Perkin. Trans. 2* 1987;(11):1609–1615.
- [10] Karotsis G, Teat SJ, Wernsdorfer W, et al. Calix[4]arene-Based Single-Molecule magnets. *Angew. Chem. Int. Ed.* 2009;48(44):8285–8288.
- [11] Morohashi N, Nanbu K, Tonosaki A, et al. Comparison of inclusion properties between p-tert-butylcalix[4]arene and p-tert-butylthiacalix[4]arene towards primary alcohols in crystals. *CrystEngComm.* 2015;17(26):4799–4808.
- [12] Furphy BM, Harrowfield JM, Ogden MI, et al. Lanthanide ion complexes of the calixarenes. Part 4. Double inclusion by p-t-butylcalix[4]arene (H_4L). Crystal structures of $[\text{Eu}_2(\text{HL})_2(\text{dmf})_4] \cdot 7\text{dmf}$ (dmf = dimethylformamide) and $\text{H}_4\text{L} \cdot \text{dmsO}$ (dmsO = dimethyl sulfoxide). *J. Chem. Soc., Dalton Trans.* 1989;(11):2217–2221.
- [13] Sanz S, McIntosh RD, Beavers CM, et al. Calix[4]arene-supported rare earth octahedra. *Chem. Commun.* 2012;48(10):1449–1451.
- [14] Bunzli JCG, Froidevaux P, Harrowfield JM. Complexes of lanthanoid salts with macrocyclic ligands. 41. Photophysical properties of lanthanide dinuclear complexes with p-tert-butylcalix[8]arene. *Inorg. Chem.* 1993;32(15):3306–3311.
- [15] D' Alessio D, Muzzioli S, Skelton BW, et al. Luminescent lanthanoid complexes of a tetrazole-functionalised calix[4]arene. *Dalton Trans.* 2012;41(16):4736–4739.
- [16] Collins EM, Mckerverey MA, Madigan E, et al. Chemically modified calix[4]arenes. Regioselective synthesis of 1,3-(distal) derivatives and related compounds. X-Ray crystal structure of a diphenol-dinitrile. *J. Chem. Soc., Perkin Trans. 1.* 1991;(12):3137–3142.
- [17] Moris S, Silva N, Saitz C, et al. NANODECORATION OF SINGLE CRYSTALS OF 5,11,17,23-TETRA-TERT-BUTYL-25,27-BIS(CYANOMETHOXY)-26, 28-DIHYDROXYCALIX[4]ARENE. *J. Chilean Chem. Soc.* 2017;62(4):3772–3778.
- [18] Dalgarno SJ, Thallapally PK, Barbour LJ, et al. Engineering void space in organic van der Waals crystals: calixarenes lead the way. *Chem Soc Rev.* 2007;36(2):236–245.

Patil BS, Banerjee D, Atwood JL, et al. Gas sorption and storage properties of calixarenes. In: Mori

- [19] Paul KS, Banerjee D, Atwood JL, et al. Gas sorption and storage properties of calixarenes. In: Neri P, Sessler JL, Wang M-X, editors. *Calixarenes and beyond*. Cham: Springer International Publishing; 2016. p. 1037–1056.
- [20] Kane CM, Ugono O, Barbour LJ, et al. Many simple molecular cavitands are intrinsically porous (zero-dimensional pore) materials. *Chem Mater*. 2015;27(21):7337–7354.
- [21] Sheldrick G. Crystal structure refinement with SHELXL. *Acta Crystallogr. Sect. C: Cryst. Struct. Commun*. 2015;71(1):3–8.
- [22] Parsons S, Flack HD, Wagner T. Use of intensity quotients and differences in absolute structure refinement. *Acta Crystallogr. Sect. B: Struct. Sci*. 2013;69(3):249–259.